

Supplemental Material

Supplemental Methods

AAV8-Ttr-control

Detection of apoptotic or necrotic hepatocytes

Continuous BrdU labeling

BrdU and HNF4 α immunostaining

Liver cell isolation

PCR specific for R26R-EYFP with looped-out stop codon

PCR sensitivity

Quantification of EYFP-negative hepatocytes

Supplemental Figures

Supplemental Figure 1 AAV8-Ttr-Cre vector titration by dot blot and qPCR.

Supplemental Figure 2 Loop out of floxed sequences by AAV8-Ttr-Cre requires Cre.

Supplemental Figure 3 No evidence for hepatocyte death or regeneration in adult R26R or R26R-EYFP mice injected with 4×10^{11} viral genomes of AAV8-Ttr-Cre.

Supplemental Figure 4 Further evidence for efficient and specific activation of EYFP expression in hepatocytes of adult R26R-EYFP mice injected with 4×10^{11} viral genomes of AAV8-Ttr-Cre.

Supplemental Figure 5 Additional data related to acute CCl₄ intoxication.

Supplemental Figure 6 Additional data related to chronic CCl₄ intoxication.

Supplemental Figure 7 Quantification of liver progenitor cell-derived hepatocytes after chronic CCl₄ intoxication or 2/3 PH.

Supplemental Figure 8 Additional data related to BDL.

Supplemental Figure 9 Additional data related to DDC feeding.

Supplemental Figure 10 Identification of liver progenitor cell-derived hepatocytes after BDL or DDC feeding.

Supplemental Tables

Supplemental Table 1 Primary antibodies.

Supplemental Table 2 Secondary antibodies.

Supplemental References

Supplemental Methods

AAV8-Ttr-control. Vector production, titration and injection were carried out as described for AAV8-Ttr-Cre.

Detection of apoptotic or necrotic hepatocytes. The Fluorescein In Situ Cell Death Detection kit (Roche) was used for terminal deoxynucleotidyl transferase dUTP nick end labeling (TUNEL). Control mice were injected intraperitoneally with 0.5 µg/g body weight of the Fas ligand Jo2 (BD).

Continuous BrdU labeling. 5-bromo-2-deoxyuridine (BrdU; Roche) was dissolved in drinking water at a final concentration of 1 mg/ml. Glucose (10 mg/ml) was added to improve taste. The solution was vigorously mixed until BrdU was completely dissolved. BrdU water was changed daily and bottles were protected from light. Mice received BrdU water ad libitum immediately after virus or PBS injection for 5 days.

BrdU and HNF4α immunostaining. For BrdU immunostaining, frozen liver samples embedded in optimum cutting temperature compound (Tissue-Tek, Sakura Finetek) were sectioned with a Leica CM3050 S cryostat, air dried for 2 hours and fixed in acetone at -20C° for 10 minutes. Next, sections were air dried for 5 minutes, rehydrated in PBS for 5 minutes, immersed in 2 N HCl for 30 minutes and neutralized with 0.1 M NaBorate, pH 8.0 for 10 minutes. After multiple H₂O rinses, sections were washed in PBS 3 times, blocked in 10% serum for 1 hour and incubated with primary antibody at 37C° for 1 hour and secondary antibody at room temperature for 1 hour (Supplemental Tables 1 and 2). Nuclear DNA was stained with 300 nM DAPI

(Millipore). HNF4 α immunostaining of paraffin-embedded liver sections was carried out using the M.O.M. kit (Vector).

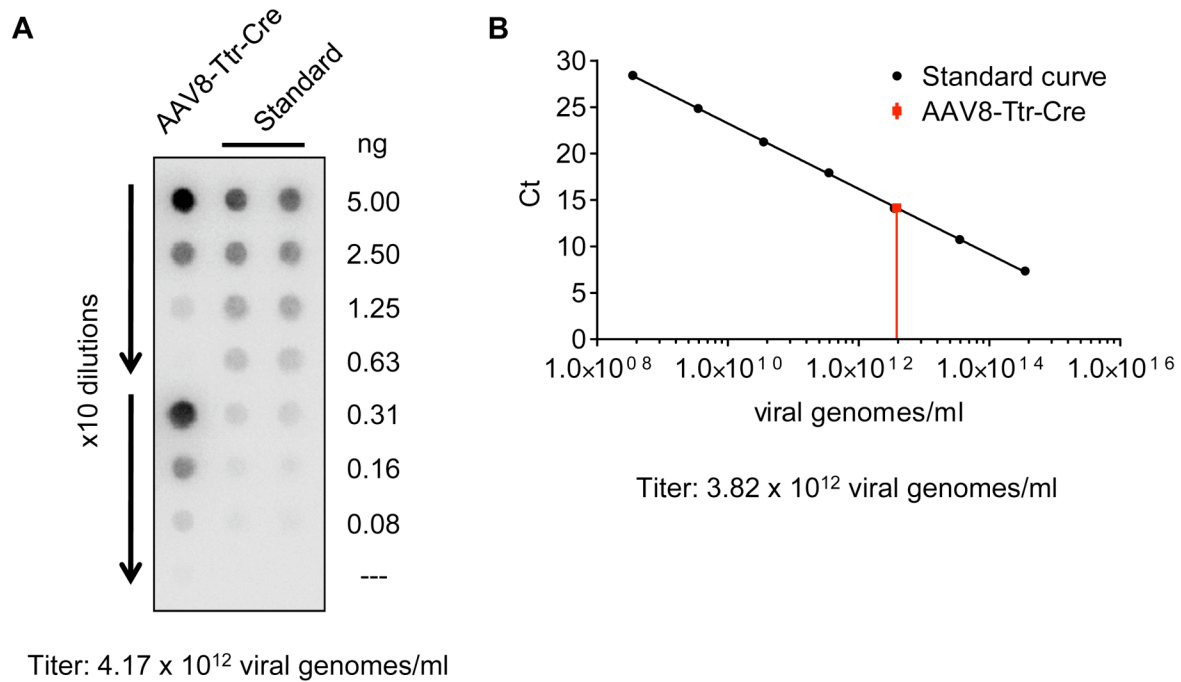
Liver cell isolation. Primary mouse liver cell suspensions were prepared and fractionated on a FACSAria II cell sorter (BD) as previously described (1).

PCR specific for R26R-EYFP with looped-out stop codon. Genomic DNA was extracted with the QIAamp DNA Blood Mini kit (Qiagen). DNA concentration was measured with a NanoDrop 2000c (Thermo Scientific). PCR was run on a ViiA 7 system (Applied Biosystems) at 50°C for 2 minutes, 95°C for 10 minutes followed by 40 cycles at 95°C for 15 seconds and 60°C for 1 minute and 15 seconds. PCR products were visualized in a 1.5% agarose gel containing 0.5 μ g/ml ethidium bromide (both Fisher Scientific) with a BioImaging Systems BioDoc-It system. Primer sequences were: R26R-EYFP forward AAAGTCGCTCTGAGTTGTTAT and reverse GAACTTGTGGCCGTTTACGTC; *Gapdh* forward TGTTGAAGTCACAGGAGACAACCT and reverse AACCTGCCAAGTATGATGACATCA.

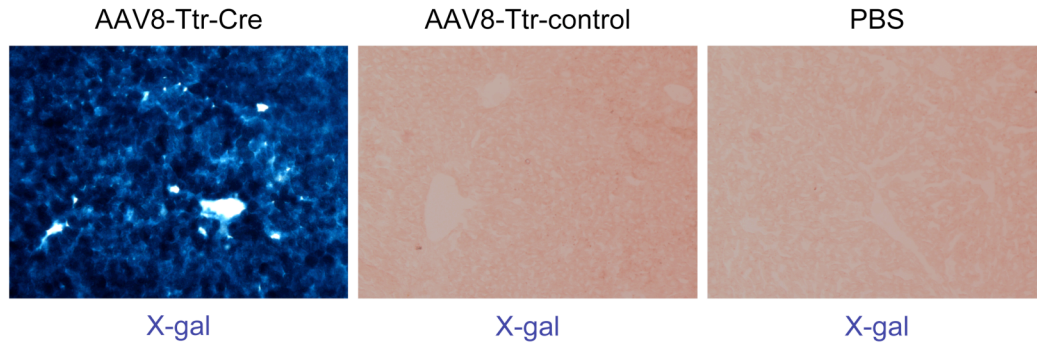
PCR sensitivity. The number of cells carrying R26R-EYFP with looped-out stop codon that could be detected with the PCR was determined as follows: The amplicon from 1 ng of DNA extracted from whole liver of a 10-week-old male Alb-Cre, R26R-EYFP mouse was readily detectable (Supplemental Figure 4D). Considering that (a) the mouse genome has 2.72×10^9 bp (2), (b) the molecular weight of 1 bp is 660 daltons and (c) 1 dalton is 1.67×10^{-12} pg, a 1n mouse cell contains $a \times b \times c = 3$ pg of DNA, whereas a 2n mouse cell contains 6 pg of DNA. The R26R-EYFP stop codon is looped out in both hepatocytes and biliary cells in Alb-Cre,

R26R-EYFP mice, which comprise approximately 60% and 5% of the liver cells, respectively (3). Thus, in 1 ng of total liver DNA, 600 pg are derived from hepatocytes and 50 pg are derived from biliary cells. The ploidy distribution of hepatocytes in the liver of a 10 week-old male mouse is 57% 4n, 40% 2n and 3% 8n (4), or approximately 60% 4n and 40% 2n. Considering that a 2n hepatocyte contains 6 pg of DNA and a 4n hepatocyte contains 12 pg of DNA, 600 pg of DNA derived from hepatocytes correspond to $(600 \text{ pg DNA} \times 0.6)/12 \text{ pg DNA/cell} + (600 \text{ pg DNA} \times 0.4)/6 \text{ pg DNA/cell} = 70$ cells, whereas 50 pg of DNA derived from biliary cells, which are all 2n, correspond to $50 \text{ pg DNA}/6 \text{ pg DNA/cell} = 8$ cells. Thus, 1 ng of DNA from whole Alb-Cre, R26R-EYFP mouse liver contains 78 cells carrying R26R-EYFP with looped-out stop codon, which is the detection limit of the PCR. 40 ng of DNA from biliary cells isolated by FACS correspond to $4 \times 10^4 \text{ pg DNA}/6 \text{ pg DNA/cell} = 6,666$ cells.

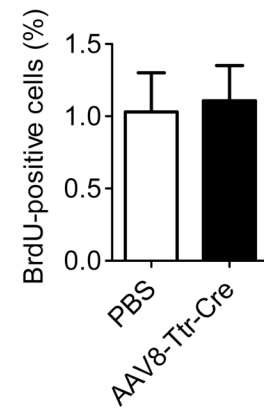
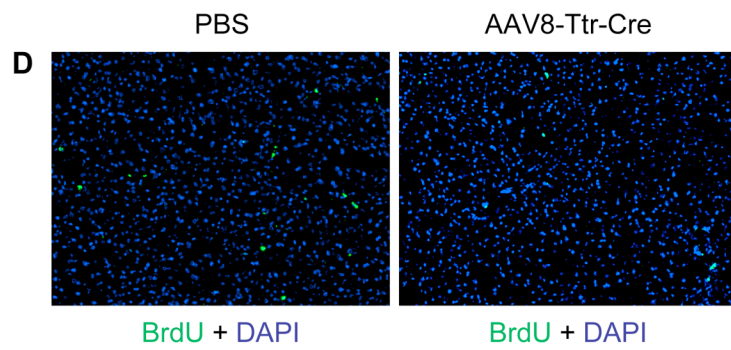
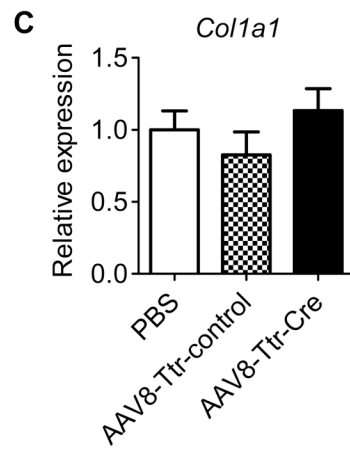
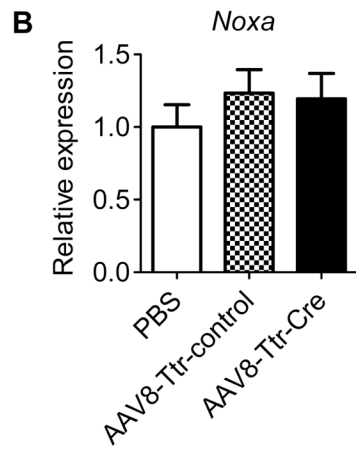
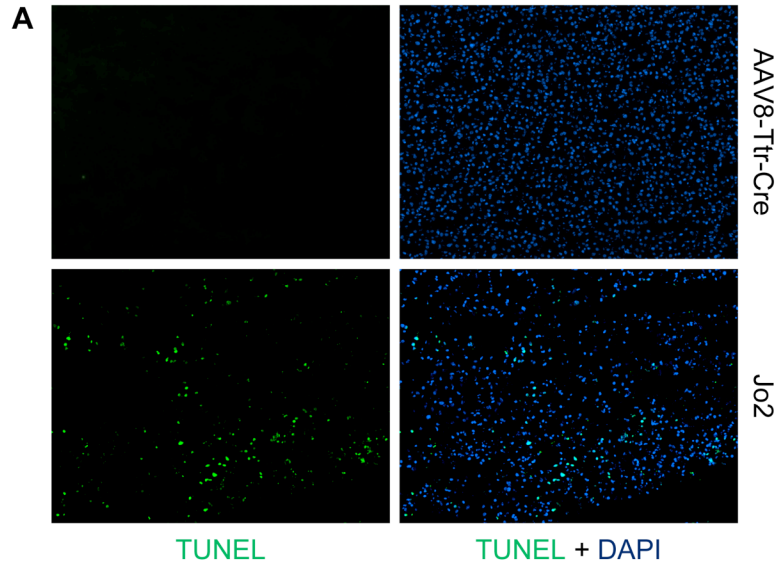
Quantification of EYFP-negative hepatocytes. The overall number of hepatocytes per field of a liver section was determined based on MUP and DAPI staining. Fields were randomly chosen. The number of MUP-positive cells that were also EYFP positive was subtracted from the overall number, the difference being EYFP-negative hepatocytes not derived from preexisting EYFP-positive hepatocytes. The percentage of EYFP-negative hepatocytes was calculated by dividing the number of EYFP-negative hepatocytes by the overall number of hepatocytes.



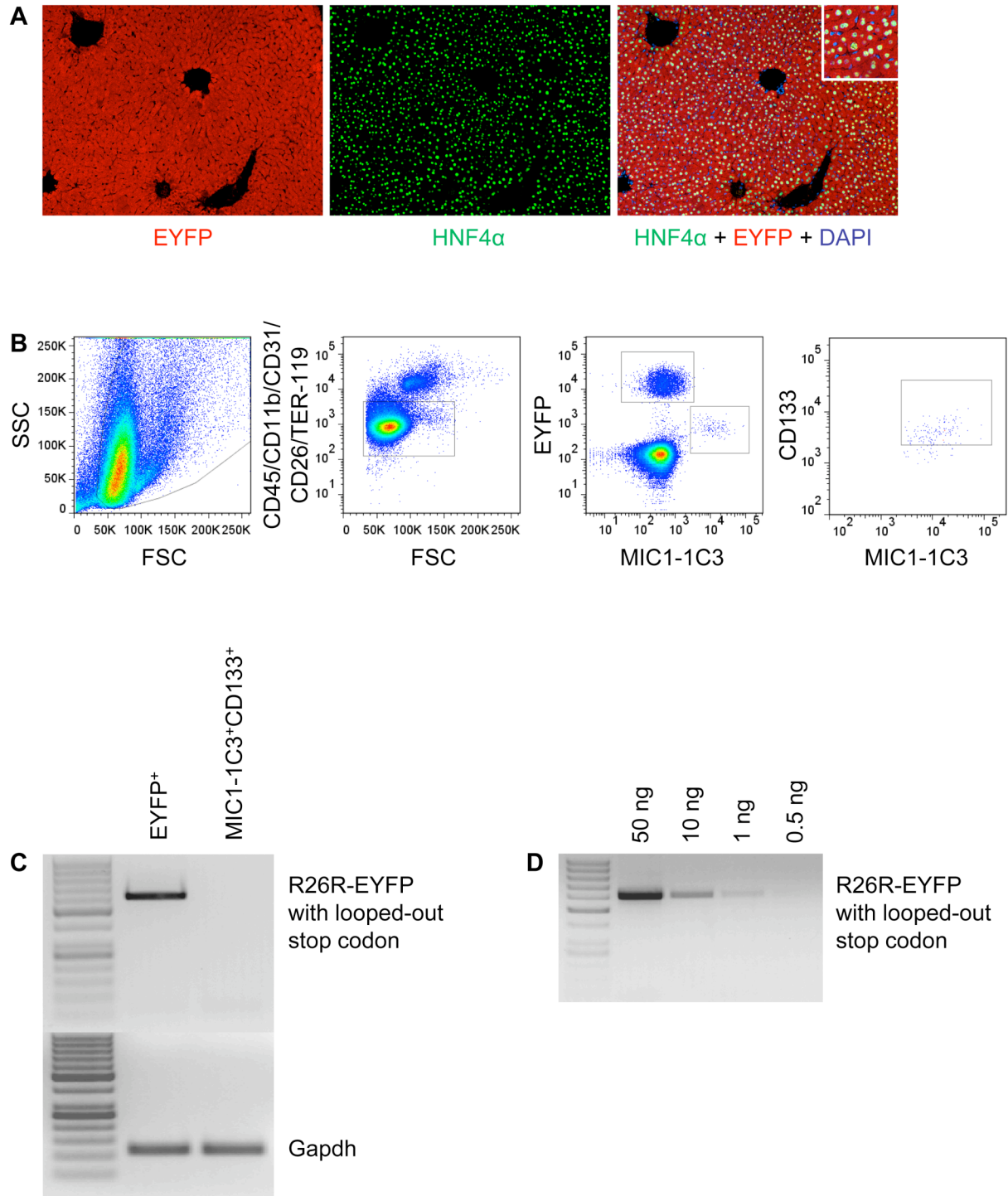
Supplemental Figure 1 AAV8-Ttr-Cre vector titration by dot blot and qPCR. **(A)** Titration by dot blot. 2 serial x10 dilutions of the vector were spotted onto a nylon membrane next to a standard consisting of 2 serial x2 dilutions of the original plasmid used for vector production. The viral titer was determined by hybridization with a radioactively labeled Ttr probe, followed by scanning and quantification. **(B)** Titration by qPCR. Viral DNA was quantified by qPCR using primers specific for the Ttr promoter. The viral titer was deduced from a standard curve generated in parallel using the original vector plasmid (shown are calculated viral genomes/ml plotted against the Ct values).



Supplemental Figure 2 Loop out of floxed sequences by AAV8-Ttr-Cre requires Cre. Adult R26R mice were injected with 4×10^{11} viral genomes of AAV8-Ttr-Cre or AAV8-Ttr-control or PBS and livers were analyzed 5 days later. X-gal staining shows that the β -gal marker gene is activated in all hepatocytes in AAV8-Ttr-Cre-injected mice, but not in any hepatocyte in mice injected with AAV8-Ttr-control or PBS. Original magnification, x100. At least 15 liver sections from 3 mice were analyzed for each experiment.

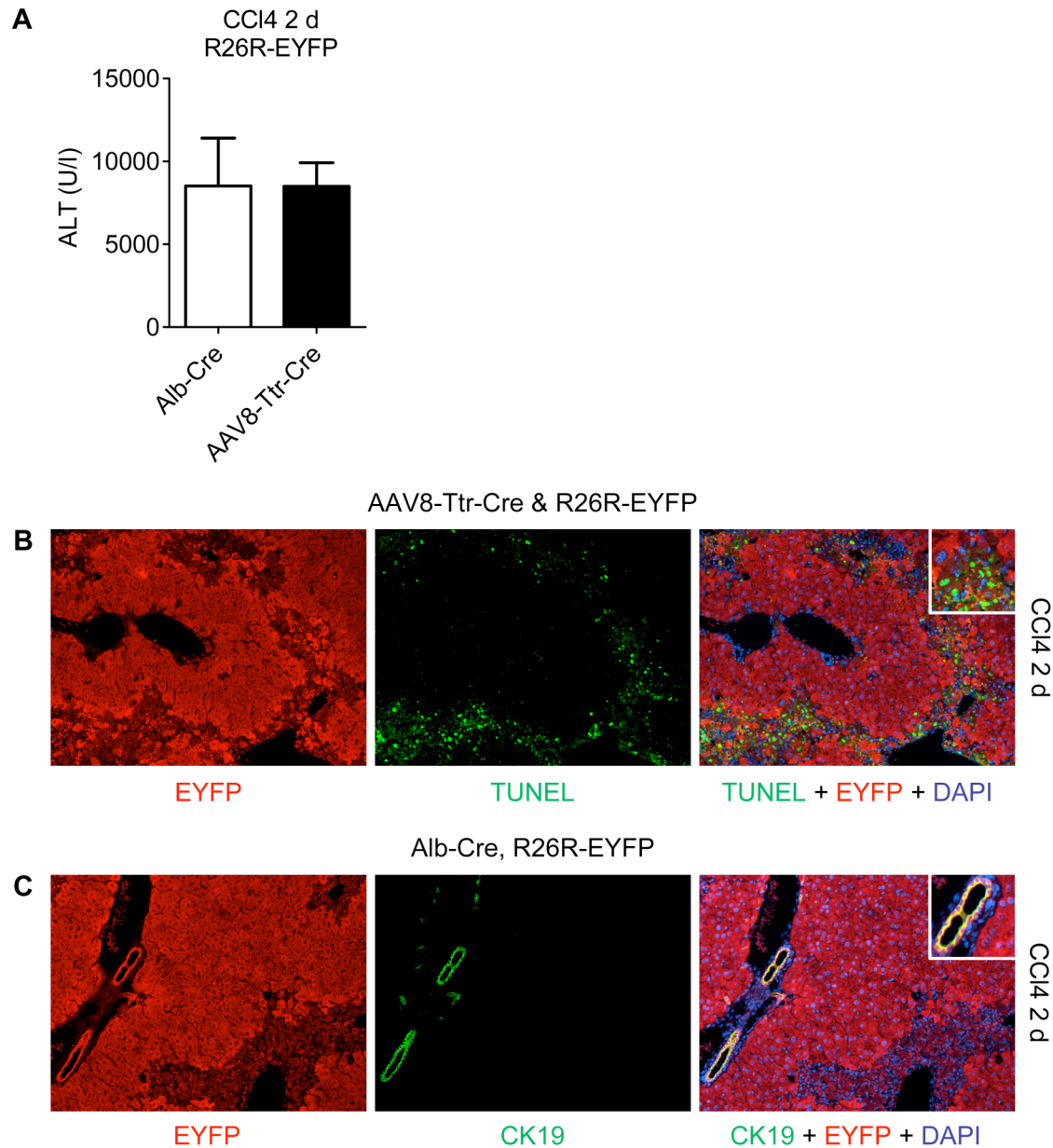


Supplemental Figure 3 No evidence for hepatocyte death or regeneration in adult R26R or R26R-EYFP mice injected with 4×10^{11} viral genomes of AAV8-Ttr-Cre. **(A)** TUNEL shows no apoptotic or necrotic cells in the liver of an R26R mouse 5 days after injection with AAV8-Ttr-Cre. The liver of an R26R mouse injected with the Fas ligand Jo2 contains many apoptotic cells (green). 12 liver sections from 4 mice were analyzed for each experiment. **(B and C)** qRT-PCR analysis shows that the proapoptotic gene *Noxa* **(B)** and the profibrotic gene *Colla1* **(C)** are not induced in livers of R26R-EYFP mice 5 days after injection with AAV8-Ttr-Cre. 4 mice were analyzed per group. **(D)** Continuous BrdU labeling for 5 days after injection of AAV8-Ttr-Cre or PBS into R26R-EYFP mice shows similarly small numbers of proliferating hepatocytes (green), which indicates that hepatocyte turnover is normal in AAV8-Ttr-Cre-injected mice. At least 15 liver sections from 3 mice were analyzed for each experiment. Nuclei were stained with DAPI (blue). Original magnification, x100. Data represent mean \pm SEM.



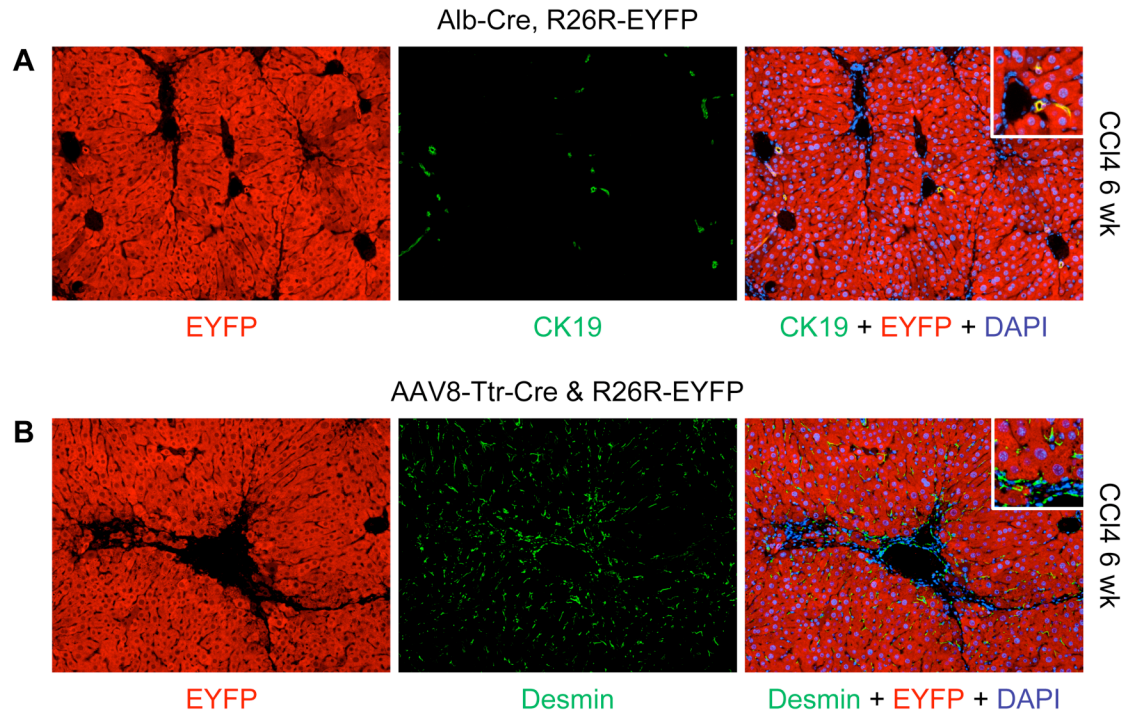
Supplemental Figure 4 Further evidence for efficient and specific activation of EYFP expression in hepatocytes of adult R26R-EYFP mice injected with 4×10^{11} viral genomes of AAV8-Ttr-Cre. (A) Coimmunostaining shows that all cells positive for the hepatocyte-specific

marker HNF4 α (green) are also positive for EYFP (red) 5 days after injection. Nuclei were stained with DAPI (blue). Original magnification, x100, inset x200. 15 liver sections from 3 mice were analyzed. **(B)** Isolation of hepatocytes and biliary cells enriched for liver progenitor cells from AAV8-Ttr-Cre-injected R26R-EYFP mice by FACS. Debris, granulocytes, macrophages, endothelial cells, erythrocytes and some hepatocytes were excluded from liver cell suspensions by FSC/SSC gating and based on expression of the cell surface markers CD45, CD11b, CD31, TER-119 and CD26. Biliary cells were identified by expression of the duct cell surface marker MIC1-1C3 and enriched for liver progenitor cells based on CD133 expression (1). Hepatocytes were identified by EYFP expression. No MIC1-1C3⁺EYFP⁺ cells were detected, indicating that AAV8-Ttr-Cre does not activate the R26R-EYFP marker gene in biliary epithelial cells and liver progenitor cells. **(C)** EYFP⁺ cells and MIC1-1C3⁺CD133⁺ cells depleted of CD45⁺CD11b⁺CD31⁺TER-119⁺CD26⁺ cells were analyzed by PCR specific for R26R-EYFP with looped-out stop codon. 40 ng of DNA from MIC1-1C3⁺CD133⁺ cells, corresponding to 6,666 cells (see Supplemental Methods), were negative, whereas 40 ng of DNA from EYFP⁺ cells were positive. **(D)** To specifically rule out loop out of the floxed stop codon in R26R-EYFP in liver progenitor cells, the PCR sensitivity was determined. Considering that the frequency of liver progenitor cells is 1/34.3 in CD45⁻CD11b⁻CD31⁻TER-119⁻CD26⁻MIC1-1C3⁺CD133⁺ cells (1), 6,666 of these cells contain 194 liver progenitor cells. As is evident from analysis of serial dilutions of DNA from Alb-Cre, R26R-EYFP liver, the PCR would have detected 78 liver progenitor cells (1 ng DNA; see Supplemental Methods) carrying R26R-EYFP with looped-out stop codon.

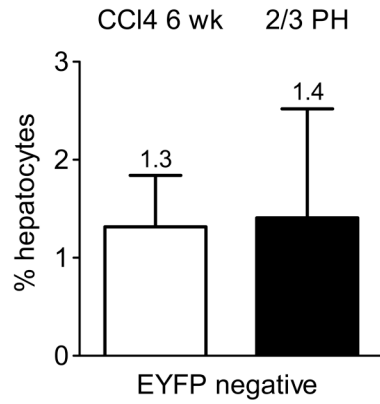


Supplemental Figure 5 Additional data related to acute CCl₄ intoxication. **(A)** Blood ALT levels reflect massive hepatocyte necrosis in Alb-Cre, R26R-EYFP and AAV8-Ttr-Cre-injected R26R-EYFP mice 2 days after CCl₄ injection. 4 mice were analyzed per group. Data represent mean \pm SEM. **(B)** TUNEL confirms pericentral necrosis in AAV8-Ttr-Cre-injected R26R-EYFP mice after acute CCl₄ intoxication. **(C)** Coimmunostaining for EYFP (red) and CK19 (green) of livers of Alb-Cre, R26R-EYFP mice after acute CCl₄ intoxication shows loss of EYFP-positive hepatocytes in pericentral areas as observed in AAV8-Ttr-Cre-injected R26R-EYFP mice

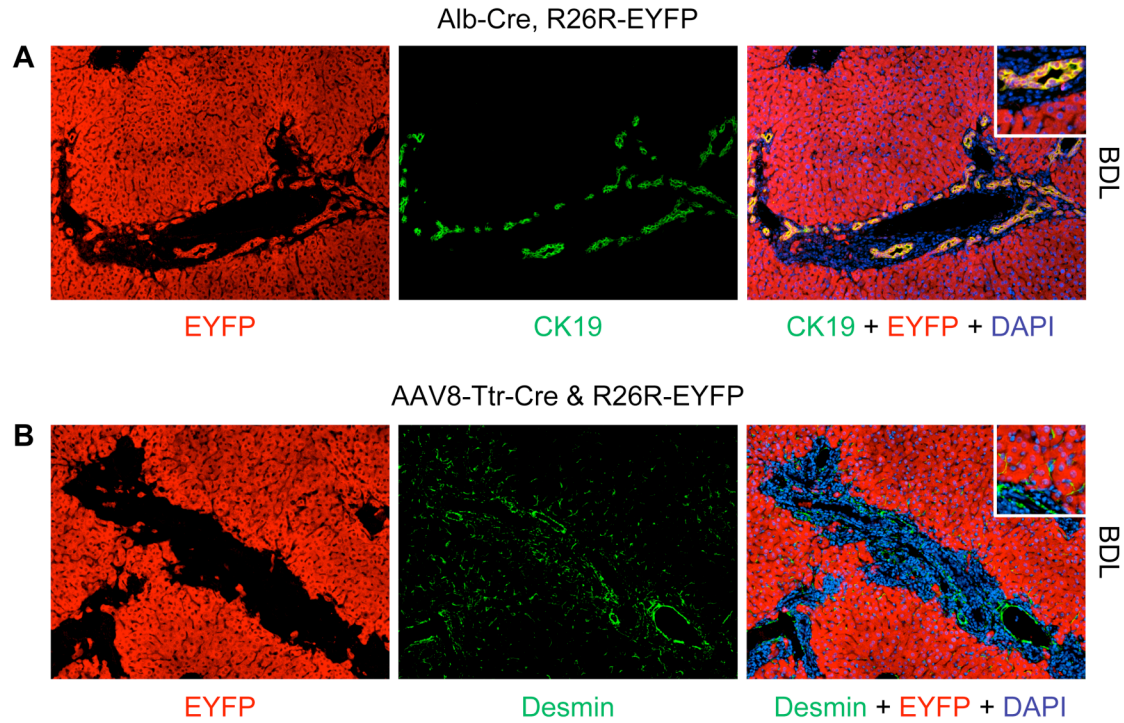
(Figure 5C). This finding excludes the possibility that the EYFP-negative, but weakly MUP-positive pericentral areas present in AAV8-Ttr-Cre-injected R26R-EYFP mice after acute CCl₄ intoxication (Figure 5D) contain liver progenitor cell-derived hepatocytes because they would express EYFP in Alb-Cre, R26R-EYFP mice. Nuclei were stained with DAPI (blue). Original magnification, x100, insets x200. At least 15 liver sections from 3 mice were analyzed for each experiment.



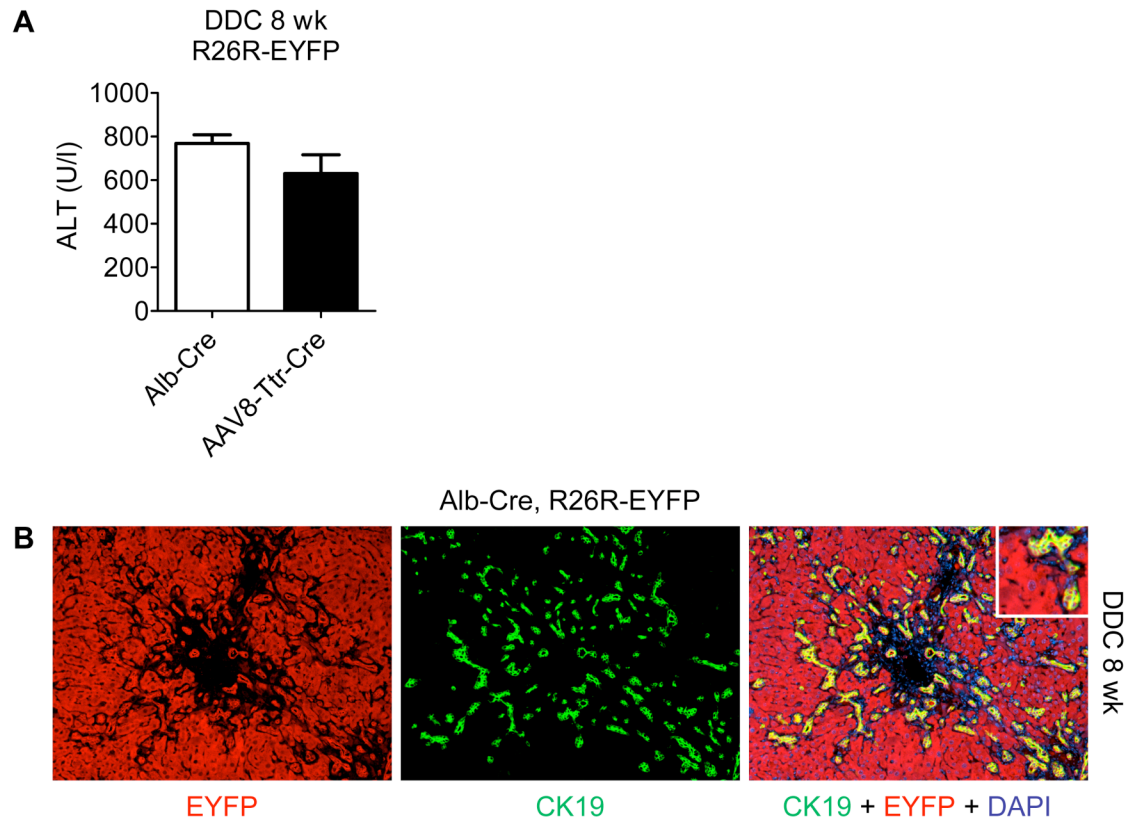
Supplemental Figure 6 Additional data related to chronic CCl₄ intoxication. **(A)** Coimmunostaining for EYFP (red) and CK19 (green) of livers of Alb-Cre, R26R-EYFP mice after chronic CCl₄ intoxication fails to detect clusters of EYFP-negative hepatocytes as observed in AAV8-Ttr-Cre-injected R26R-EYFP mice (Figure 6C). **(B)** Coimmunostaining for EYFP (red) and Desmin (green) of livers of AAV8-Ttr-Cre-injected R26R-EYFP mice after chronic CCl₄ intoxication shows a large number of Desmin-positive cells, none of which coexpresses EYFP. Nuclei were stained with DAPI (blue). Original magnification, x100, insets x200. At least 15 liver sections from 3 mice were analyzed for each experiment.



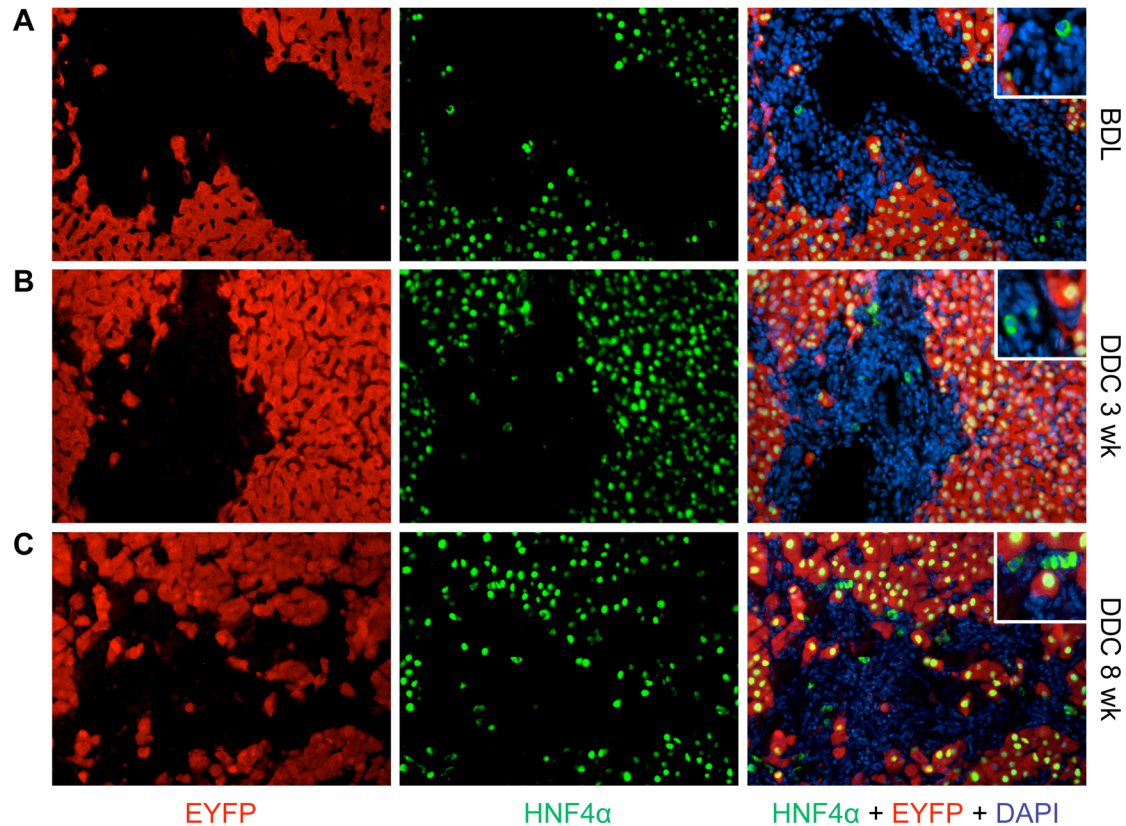
Supplemental Figure 7 Quantification of liver progenitor cell-derived hepatocytes after chronic CCl4 intoxication or 2/3 PH. The percentage of EYFP-negative hepatocytes found in AAV8-Ttr-Cre-injected R26R-EYFP mice after 6 weeks of CCl4 intoxication or 2/3 PH is given. Approximately 5,000 hepatocytes in at least 15 liver sections from 3 mice were analyzed for each experiment.



Supplemental Figure 8 Additional data related to BDL. **(A)** Coimmunostaining for EYFP (red) and CK19 (green) of livers of Alb-Cre, R26R-EYFP mice after BDL shows expansion of biliary cells, which are all double positive (yellow). **(B)** Coimmunostaining for EYFP (red) and Desmin (green) of livers of AAV8-Ttr-Cre-injected R26R-EYFP mice after BDL shows a large number of Desmin-positive cells, none of which coexpresses EYFP. Nuclei were stained with DAPI (blue). Original magnification, x100, insets x200. At least 15 liver sections from 3 mice were analyzed for each experiment.



Supplemental Figure 9 Additional data related to DDC feeding. **(A)** Blood ALT levels indicate hepatocyte injury in Alb-Cre, R26R-EYFP and AAV8-Ttr-Cre-injected R26R-EYFP mice after 8 weeks of DDC feeding. 4 mice were analyzed per group. Data represent mean \pm SEM. **(B)** Coimmunostaining for EYFP (red) and CK19 (green) of livers of Alb-Cre, R26R-EYFP mice after 8 weeks of DDC feeding shows expansion of biliary cells, which are all double positive (yellow). Nuclei were stained with DAPI (blue). Original magnification, x100, inset x200. 15 liver sections from 3 mice were analyzed.



Supplemental Figure 10 Identification of liver progenitor cell-derived hepatocytes after BDL or DDC feeding. (A-C) Coimmunostaining for EYFP (red) and HNF4 α (green) of livers of AAV8-Ttr-Cre-injected R26R-EYFP mice after BDL (A) or 3 (B) or 8 (C) weeks of DDC feeding. EYFP-negative and HNF4 α -positive cells are cells committed to the hepatocyte fate that are not derived from preexisting hepatocytes, which suggests that they are hepatocytes derived from liver progenitor cells. Nuclei were stained with DAPI (blue). Original magnification, x200, insets x400. At least 15 liver sections from 3 mice were analyzed for each experiment.

Supplemental Table 1 Primary Antibodies

Antigen	Species	Dilution	Supplier
α -SMA	Rabbit	1/100	Abcam
BrdU	Rat	1/50	Abcam
CD11b-PE	Rat	1/200	BD
CD26-PE	Rat	1/100	BioLegend
CD31-PE	Rat	1/100	eBioscience
CD45-PE	Rat	1/400	BD
CD133-PerCP-eFluor 710	Rat	1/100	eBioscience
CK19	Rabbit	1/100	Abdomax
Desmin	Goat	1/100	R&D
F4/80	Rat	1/100	Serotec
GFAP	Rabbit	1/100	Dako
GFP	Chicken	1/200	Abcam
HNF4 α	Mouse	1/100	Abcam
Isolectin B4	Biotinylated	1/100	Vector
MIC1-1C3	Rat	1/20	Markus Grompe
MUP	Goat	1/200	Cedarlane
TER-119-PE	Rat	1/200	BD

Supplemental Table 2 Secondary Antibodies

Reactivity	Species	Fluorochrome	Dilution	Supplier
Chicken	Donkey	DyLight 549	1/200	Jackson Immunoresearch
Goat	Donkey	Alexa Fluor 488	1/200	Molecular Probes
Mouse	Rabbit	HRP	1/100	Jackson Immunoresearch
Rabbit	Donkey	DyLight 488	1/200	Jackson Immunoresearch
Rat	Donkey	DyLight 488	1/200	Jackson Immunoresearch
Rat	Goat	APC	1/200	BD
Streptavidin		DyLight 488	1/100	Jackson Immunoresearch

Supplemental References

1. Dorrell, C., Erker, L., Schug, J., Kopp, J.L., Canaday, P.S., Fox, A.J., Smirnova, O., Duncan, A.W., Finegold, M.J., Sander, M., et al. 2011. Prospective isolation of a bipotential clonogenic liver progenitor cell in adult mice. *Genes Dev* 25:1193-1203.
2. Waterston, R.H., Lindblad-Toh, K., Birney, E., Rogers, J., Abril, J.F., Agarwal, P., Agarwala, R., Ainscough, R., Alexandersson, M., An, P., et al. 2002. Initial sequencing and comparative analysis of the mouse genome. *Nature* 420:520-562.
3. Malarkey, D.E., Johnson, K., Ryan, L., Boorman, G., and Maronpot, R.R. 2005. New insights into functional aspects of liver morphology. *Toxicol Pathol* 33:27-34.
4. Shima, A., and Sugahara, T. 1976. Age-dependent ploidy class changes in mouse hepatocyte nuclei as revealed by Feulgen-DNA cytofluorometry. *Exp Gerontol* 11:193-203.